Integrated Quasi-Phase-Matched Second-Harmonic Generator and Electrooptic Scanner on $LiTaO_3$ Single Crystals

Venkatraman Gopalan, Matthew J. Kawas, Mool C. Gupta,
T. E. Schlesinger, *Senior Member, IEEE,* and Daniel D. Stancil, *Senior Member, IEEE*

***Abstract*—We report the first integrated quasi-phase-matched second-harmonic generator and electrooptic scanner on ferroelectric Z-cut $LiTaO_3$. The quasi-phase-matched second-harmonic generation device frequency doubles the infrared light at 829.7 nm into blue at 414.85 nm with a bulk coversion efficiency of 0.52%/W-cm. The blue light generated in the bulk then passes through an electrooptic scanner, consisting of a series of lithographically defined triangular-shaped domain-inverted regions extending through the thickness of the crystal. A deflection of 12 mrad/kv for the output blue light and 7.4 mrad/kv for the infrared light was observed at the scanner output.**

THE DEVELOPMENT of solid state blue laser sources is being actively pursued employing quasi-phase-matched second-harmonic generation (QPM-SHG) in $LiTaO_3$ crystals. A blue laser source integrated with high-speed scanning capability is of interest for a variety of applications including optical data storage and laser printing. In optical data storage, for example, a shorter wavelength (doubling from infrared to blue) will increase the areal data storage on optical disks by four times, and the ability to scan the laser beam nonmechanically at high speeds will greatly enhance tracking and data access.

In this letter, we report the first successful integration of a QPM-SHG and an electrooptic scanner on the same $LiTaO_3$ wafer. We show that such an integration is naturally compatible from both design and fabrication aspects.

Fig. 1 shows the schematic of the integrated device. The first half (on the left, 7.8 mm in length) of the device is a quasi-phase-matched second-harmonic generation device. It consists of a periodic domain inverted grating with a period of $\Lambda = 3.5$ μm with a phase-matching infrared wavelength of $\lambda = 2\Lambda[n_e^{2\omega} - n_e^{\omega}] = 829.7$ nm, where n_e is the extraordinary refractive index at frequency ω and 2ω. An infrared beam is focused at the center of the SHG grating in the bulk of the crystal, using a microscope objective with a numerical aperture of approximately 0.015 N. A. With this arrangement, the beam stays within the top 200 μm near the surface of the crystal where the periodic domain grating is very uniform. The beam also propagates through the entire length of the device (~15 mm) without exiting the surface. The polarization of the infrared and the blue light is TM with the electric field along the c axis of the crystal.

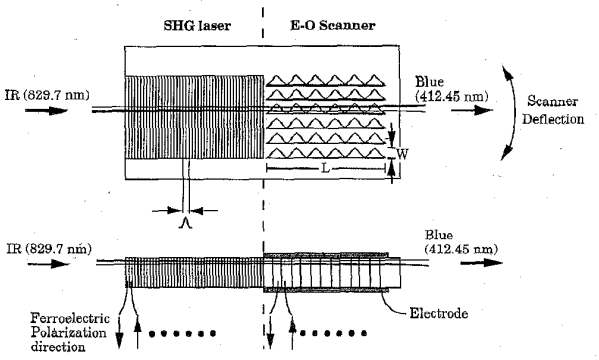

Fig. 1. A schematic of the integrated QPM-SHG with electrooptic scanners on Z-cut $LiTaO_3$ crystals. The top view (top) and cross section (bottom) are shown.

The blue light generated in the SHG region then propagates through an electrooptic scanner. The scanner consists of a series of domain-inverted triangular prisms (each triangle length l, width, W) in the crystal [1]. The total scanner length is $L = nl$, where, n is the number of triangular prisms. The index difference Δn_e between the domain inverted prism regions and the surrounding crystal can be controlled by applying a uniform electric field, E_z across the crystal and is given by $\Delta n_e = n_e^3 r_{33} E_z$, where n_e is the extraordinary index n_e, and r_{33} is the electrooptic coefficient. The subscripts 3 and z denote the direction along the polarization axis of the crystal. When the blue light exits the crystal, it is deflected by an angle $\theta = \Delta n_e L/W$ [2]. The fabrication process is described below.

Room-temperature electric-field poling of chemically patterned surfaces was employed for the fabrication of both the scanner and the SHG grating as detailed elsewhere [3]. Hence, the fabrication of the entire integrated device was carried out with one integrated process. The $LiTaO_3$ crystals,

Manuscript received July 3, 1996. This work was supported in part by the Advanced Technology Program of the Department of Commerce through a cooperative grant to the National Storage Industry Consortium (NSIC) and by the National Science Foundation under Grant ECD-8907068.

V. Gopalan is with the Center for Materials Science, Los Alamos National Laboratory, Los Alamos, NM 87545 USA.

M. J. Kawas, T. E. Schlesinger, and D. D. Stancil are with the Data Storage Systems Center, Carnegie Mellon University, Pittsburgh, PA 15213 USA.

M. C. Gupta is with Imaging Research and Advanced Development, Eastman Kodak Company, Rochester, NY 14650-2017 USA.

Publisher Item Identifier S 1041-1135(96)08776-9.

obtained from Yamaju Inc. (Japan), were of optical grade. Using photolithography, a periodic ($\Lambda = 3.5$ μm) Ta metal grating (for the SHG) and triangular Ta regions (for the scanner), as depicted in Fig. 1, were defined on the c^-face of an approximately 0.5 mm thick Z-$LiTaO_3$ crystal. The Ta film was 500 Å thick. The crystal was then heated in pyrophosphoric acid at 260 °C for 50 min. This causes proton exchange [4] (diffusion of protons into the crystal) in the regions not covered by the tantalum metal and increases the electric field required to reverse the polarization in these regions. The sample was then cooled to room temperature and cleaned with water. Following this, an electric field of about 21 kv/mm was applied to the region where the scanner is defined. For this purpose, the original Ta film on the c^-face was used as one electrode and a uniform liquid electrode (saturated KNO_3 solution in water) on the c^+ surface. Thus, domains are inverted only under the Ta metal, defining triangular domain inverted prism regions through the thickness of the crystal.

The Ta metal was then stripped off the entire device by dipping it for ~10 s in a mixture of 1 part HF with 2 part HNO_3 at room temperature. Next, using two liquid electrode columns (with electrode area A) across the SHG region of the device, an electric field of ~21 kv/mm was applied and the domain reversal process monitored using transient current measurements [3]. The poling process was carried out until the total charge under the current peak equaled P_sA, where $P_s = 50$ μC/cm^2 for $LiTaO_3$ crystals [5]. This causes only the crystal between the proton exchanged regions to reverse its polarization, thus giving a 3.5 μm period domain grating in the SHG region. Because the device described here operates in the bulk configuration, it is not necessary to anneal the final device above 400 °C to remove the surface proton exchanged layer (~0.5 μm). The ends of the sample were polished for optical coupling and Au–Cr electrodes were deposited on the C^- and C^+ faces of the crystal in the scanner region for applying a uniform electric field.

Fig. 2 presents the performance of the SHG device in bulk configuration as described in Fig. 1. The phase-matching infrared wavelength was found to be 829.7 nm. For a 7.8 mm SHG device length, 26 μW of blue light was obtained with 80 mW of infrared light focused into the device. This gives a bulk efficiency of 0.52%/W-cm. Upon applying an electric field across the scanner, both the blue and the infrared light deflect at the output of the crystal. This was imaged on a piece of paper. Fig. 3 is a double exposure photograph of the deflected blue beam for an applied voltage of ±750 V. The measured deflections were 12 mrad/kv for the blue light and 7.4 mrad/kv for the infrared beam. For a crystal thickness of 474 μm and the electrooptic coefficient of 30.5 pm/V (reported at 633 nm), [6] the expected index difference between the domain inverted prisms and the surrounding crystal is $\Delta n = 7.55 \times 10^{-4}$ for an applied voltage of 1 kv voltage at 414.85 nm. This gives a theoretical estimate [2] of $\theta = \Delta nL/W = 9$ mrad, where $L = 6$ mm and $W = 0.5$ mm was used. This estimate is smaller than the measured deflection of 12 mrad/kv observed for the blue light. Similarly, the theoretical estimate at 829.7 nm is $\Delta n = 6.43 \times 10^{-4}$ for an applied voltage of 1 kv, which gives a deflection angle of $\theta = 7.72$ mrad. This is

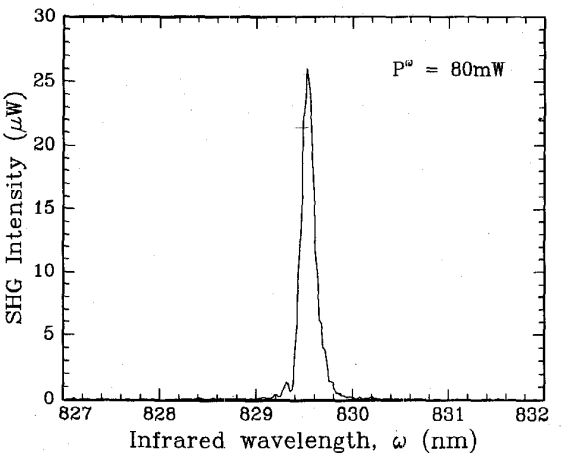

Fig. 2. The second-harmonic generation (SHG) intensity versus phase-matched infrared wavelength.

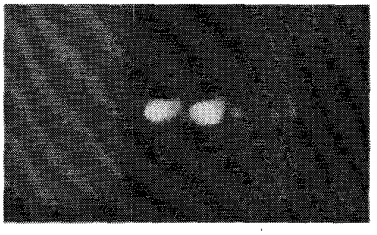

Fig. 3. A double exposure photograph of the deflected blue light (414.85 nm) with −750 V (left spot) and +750 V (right spot) applied across the scanner in the integrated device. The Z-cut $LiTaO_3$ crystals was 0.474 mm thick. The deflection angle is 18 mrad.

closer to the measured deflection angle of 7.4 mrad/kv for the infrared beam. Since the deflection, $\theta = \Delta n_e L/W$, the discrepancy between the observed and theoretical deflection at 414.85 nm can be due to error in n_e, E_z, r_{33}, L, or W. The values of L, W, and E_z were measured within a few percent error. The values of n_e as a function of wavelength for single crystal $LiTaO_3$ were taken from literature, [7] reported for single crystal $LiTaO_3$. One possible explanation for why the scanner deflection is close to theoretical estimate at infrared wavelength but significantly different at blue wavelength is the possible dispersion in the electrooptic coefficient with the wavelength of light. This suggestion is plausible since a considerable dispersion of r_{22} for structurally similar $LiNbO_3$ has also been reported [8] in the visible range. The optical dispersion of r_{33} is currently under investigation.

We shall now summarize the advantages and disadvantages of the above design. To our knowledge, this is the first demonstration of an integrated QPM-SHG and an electrooptic scanner on the same chip. The processes for the fabrication of the laser and the scanner have been shown to be compatible. The device is compact (only ~15-mm total length). The scanner consumes negligible power and is believed to be capable of high speed (100 MHz and higher) operation. We have tested similar scanners up to 10 MHz with no observable decrease in deflection sensitivity.

A limitation of the present design of this integrated device is that the SHG is through the bulk of the crystal, and

therefore high blue powers cannot be achieved. Also, because the IR beam is focused at the center of the SHG region, the beam is diverging when it passes through the scanner. This strongly limits the number of resolvable spots (N) at the output since N = (deflection angle)/(divergence angle) [2]. An improved design would use channel waveguides in the SHG region for high conversion efficiencies and hence blue power, along with a planar waveguide in the scanner region to allow deflection in the x-y plane of the crystal. However, a channel waveguide will further increase the divergence of the blue light at the end of the SHG region, and so integrated lenses would be required between the laser and scanner. Some lenses on $LiNbO_3$ crystals using double proton exchange technique have been reported, [9] and we are also in the process of designing electrooptic lenses using domain inversion.

In conclusion, we report the first integrated optical device on ferroelectric Z-cut $LiTaO_3$ crystal consisting of a quasi-phase-matched second-harmonic generation section and an electrooptic beam deflector on the same chip. Blue light at 414.85 nm was generated in the bulk of the crystal with an efficiency of 0.52%/W-cm. It then passes through an electrooptic scanner comprised of a series of triangular prism-shaped domain-inverted regions through the thickness of the crystal. A deflection of 12 mrad/kv for the output blue light and 7.4 mrad/kv for the infrared light was observed at the scanner output.

The authors would like to acknowledge the help of Dr. V. Wang and P. Mack at Eastman Kodak Company, and J. Li at Carnegie Mellon University.

REFERENCES

[1] Q. Chen, Y. Chiu, D. N. Lambeth, T. E. Schlesinger, and D. D. Stancil, "Guided-wave electro-optic beam deflector using domain reversal in $LiTaO_3$," *J. Lightwave Technol.*, vol. 12, pp. 1401–1404, 1994.

[2] J. F. Lotspeich, "Electro-optic light beam deflection," *IEEE Spectrum*, vol. 5, pp. 45–53, Feb. 1968.

[3] C. Baron, H. Cheng, and M. C. Gupta, "Domain inversion in $LiTaO_3$ and $LiNbO_3$ by electric field application on chemically patterned crystals," *Appl. Phys. Lett.*, vol. 68, no. 4, pp. 481–483, 1996.

[4] K. El Haldi, P. Baldi, M. P. De Micheli, A. Luycuras, V. A. Fedorov, and Yu. N. Korkishko, "Control of proton exchange for $LiTaO_3$ waveguides and the crystal structure of $H_xLi_{1-x}TaO_3$," *Opt. Lett.*, vol. 20, no. 16, pp. 1698–1700, 1995.

[5] S. H. Wemple, M. Didomenico, Jr., and I. Camlibel, "Relationship between linear and quadratic electro-optic coefficients in $LiNbO_3$, $LiTaO_3$, and other oxygen-octahedra ferroelectrics based on direct measurement of spontaneous polarization," *Appl. Phys. Lett.*, Vol. 12, pp. 209–211, 1968.

[6] K. Onuki, N. Uchida, and T. Saku, "Interferometric method for measuring electro-optic coefficients in crystals," *J. Opt. Soc. Amer.*, vol. 62, pp. 1030–1032, 1972.

[7] W. L. Bond, "Measurement of the refractive indices of several crystals," *J. Appl. Phys.*, vol. 36, pp. 1674–1677, 1965.

[8] A. Chirakadze, S. Machavariani, A. Natsvlishvili, and B. Hvitia, "Dispersion of the linear electro-optic effect in lithium niobate," *J. Phys. D. App. Phys.*, vol. 23, no. 9, pp. 1216–1218, 1990.

[9] D. Y. Zhang and C. S. Tsai, "Single mode waveguide microlenses and microlens array fabrication in $LiNbO_3$ using titanium indiffused proton exchange technique," *Appl. Phys. Lett.*, vol. 46, pp. 703–705, 1985.